

AD-A182 427

TIME RESOLVED MEASUREMENTS OF LARGE AMPLITUDE VELOCITY
FLUCTUATIONS WITH A (U) MICHIGAN UNIV ANN ARBOR DEPT
OF AEROSPACE ENGINEERING W W WILLMARTH ET AL NOV 84
N00014-76-C-0571

1/1

UNCLASSIFIED

F/G 14/2

NL

						END						
						8-87						
						DTIC						



MICROCOPY RESOLUTION TEST CHART
NATIONAL BUREAU OF STANDARDS 1963-A

12

014439-03

DTIC FILE COPY

TIME RESOLVED MEASUREMENTS OF LARGE AMPLITUDE VELOCITY
FLUCTUATIONS WITH A THREE-SENSOR HOT-WIRE PROBE

W. W. Willmarth, T. Wei and K. Madnia

Sponsored by Department of the Navy
Office of Naval Research
Contract N00014-76-C-0571

Department of Aerospace Engineering
University of Michigan, Ann Arbor, Michigan 48109

November 1984

DTIC
ELECTE
JUL 15 1987
S
E
D

UNCLASSIFIED DISTRIBUTION UNLIMITED

87 7 14 014

AD-A182 427

**TIME RESOLVED MEASUREMENTS OF LARGE AMPLITUDE VELOCITY
FLUCTUATIONS WITH A THREE-SENSOR HOT-WIRE PROBE**

W. W. Willmarth, T. Wei and K. Madnia

Department of Aerospace Engineering

University of Michigan, Ann Arbor, Michigan 48109

Calibration and data reduction procedures are reported for a three sensor hot-wire probe (TSI model 1298) used to determine all three velocity components in large amplitude turbulence at a speed of 65 ft./sec. Hot-wire sensors were necessary because hot-film sensors did not produce a steady, predictable signal for a large variation of the angle between the sensor axis and the stream. A digital computer was used to obtain an iterative solution of the equations relating the sensor signals to the velocity components. Reasonably accurate measurements of the time resolved velocity components were made for transverse velocities less than approximately $2/10$ of the stream velocity. For larger transverse velocities, the instability of the iterative solution in conjunction with the occurrence of multiple solutions presents a serious problem. Improved methods of iteration and additional information beyond that provided by the three sensor signals appears to be necessary to determine the correct solution among a maximum of four possible solutions with flow downstream along the probe axis.

INTRODUCTION

This paper is a study of the problem of making time resolved measurements of all three velocity components of a highly turbulent flow using a three-sensor hot-wire probe. The literature describing the use of hot-wires and other types of heated sensors for turbulence measurements is extensive. The recent review articles by Comte-Bellot¹ and Blackwelder² and the book by Perry³ provide detailed information on the hot-wire method of measurement and an introduction to the literature. Unfortunately the problem of making accurate, time resolved measurements of all three large amplitude velocity fluctuations using three hot-wires is not treated in detail in the above review articles.

When three dimensional velocity fluctuations are encountered, the response of a single sensor is a function of all three velocity components. One must make simultaneous measurements of the output signals from at least three sensors, in order to obtain the data required to determine all three turbulent velocity components. If the turbulence level is low a linearized approximate solution of the three-sensor hot-wire response equations is possible. However, a linearized solution is not adequate for large amplitude turbulent velocity fluctuations. Digital computers fitted with suitable A/D converters are a natural choice for the simultaneous measurements and computations required for measurements of this type.

In 1974, Lakshminarayana and Poncet⁴ reported the use of an X-wire probe and a single-wire probe to measure three velocity components in a turbulent wake flow behind a turbomachinery

rotor. The data from each sensor was digitized and a digital computer was used to linearize the sensor signals thus determining the the velocity normal to each sensor. The computer was then used to solve three simultaneous equations relating the velocity normal to the sensors to the actual velocity components. Average values of the mean and fluctuating velocity components were reported and estimates of the accuracy of the results based on statistical measures for a Gaussian process were made. The method and accuracy of the solution of the three simultaneous equations and the possible occurrence of multiple roots were not documented.

In 1978, Moffat, Yavuzkurt, and Crawford⁵ developed and used a custom built analog computer to obtain the instantaneous velocity components in real time using a DISA triaxial-wire probe. In the same year, Fabris⁶ reported the development of a special four-wire probe (one wire measured temperature) and the use of a digital computer employing the Newton-Raphson technique to iteratively solve three simultaneous nonlinear hot-wire response equations in a heated turbulent wake flow.

Recently, 1983, Paulsen⁷ described a method for obtaining a solution for the three velocity components with a digital computer using a multiple, modified Newton search algorithm. Paulsen⁷ also reported the use of this method of solution for turbulence data obtained with a subminiature triple sensor probe of his own design. The accuracy of the data was not satisfactory because prong interference was a serious problem (the prong spacing was three times the prong tip diameter) but Paulsen

stated that improvements of the probe or corrections for the prong interference will be made in the future.

Chang and Adrian⁸, in 1984, described the use of the half interval method to obtain a digital, iterative solution for the response of a three wire probe to the velocity components in a high intensity turbulent flow around the potential core of a turbulent jet. Jorgensen's⁹ cooling law was used for the wire response and the probe was a standard X-wire configuration with an adjacent slanted wire. Multiple solutions of the response equation were encountered and, as the turbulence level increased, the occurrence of non-realizable and non-solvable data was documented. The time resolved solutions for the velocity components were not presented nor was it possible to compare the computed velocity components with the instantaneous velocity components to which the probe was exposed in the turbulent flow.

Wallace¹⁰ has reported the use of an array of nine hot-wire sensors for measurements of the velocity and vorticity components at a point in a turbulent flow. As might be expected, the calibration and data processing procedures were complex. According to Wallace, in a private communication, problems similar to those encountered by Chang and Adrian occurred and the measurements had to be restricted to low amplitude turbulent fluctuations to avoid serious errors in interpretation of the probe signals.



SEARCHED	INDEXED
SERIALIZED	FILED
JUN 1984	
FBI - NEW YORK	
A-1	

In the present paper the development of a three sensor probe capable of measurements of large scale, large amplitude turbulent velocity fluctuations is described. The accuracy and limitations of the calibration and data reduction procedures are studied. The results of time resolved measurements with the probe are directly compared with the actual velocity to which the probe is exposed. The probe calibration and data reduction methods have been applied to the measurement of turbulent velocity fluctuations of large scale in the atmosphere, see Willmarth¹¹.

I. EXPERIMENTAL EQUIPMENT

A. Apparatus

A three sensor probe (model 1298 manufactured by TSI) was selected for measurements of large scale, large amplitude velocity fluctuations in the turbulent flow encountered by a vehicle driven on an expressway. The probe was calibrated by pitching and yawing it in the flow in the test section of the 61 X 61 cm. wind tunnel at the Aerospace Engineering Department of the University of Michigan. A description of this wind tunnel has been given by Uberoi¹². Fig. 1 is a drawing of the probe mounted at the center of the tunnel on two model aircraft servo units (Airtronics model 94554) which are capable of a maximum angular rotation of plus or minus 60 degrees. The pitch and yaw servo signals were generated by manually rotating the shafts of two potentiometers of a servo signal generating device. The resulting angular orientation of the servo shafts, θ_p , θ_y , (see Fig. 1) was determined from the signals produced by

two additional potentiometers (not shown) mounted on each servo shaft.

The three velocity components relative to the probe, as defined in Fig. 1, are given by:

$$u = U_{\infty} \cos \theta_p \cos \theta_y \quad (1)$$

$$v = U_{\infty} \sin \theta_p \quad (2)$$

$$w = U_{\infty} \cos \theta_p \sin \theta_y \quad (3)$$

where, θ_p , is the pitch angle, θ_y , is the yaw angle and, U_{∞} , is the free stream velocity along the axis of the wind tunnel. The free stream velocity was measured with a manometer connected to static pressure taps in the settling chamber and the test section of the wind tunnel.

The probe sensors were operated in the constant temperature mode using TSI model 1054B constant temperature linearized anemometers. The linearized sensor signals along with the servo shaft pitch and yaw potentiometer signals were recorded on analog magnetic tape using a Honeywell model 5600C tape recorder which had seven frequency modulated record and reproduce channels with frequency response from zero to 5 KHz. The recorded signals, for various flow speeds and probe orientations, were reproduced and digitized using a 12 bit analog to digital converter (Analogic model 5800) controlled by a digital computer system (Data General NOVA 840). The computer system was also used to perform the computations described later in the paper.

B. Three Sensor Probe

Fig. 2 is a sketch of the three sensor probe (TSI model 1298) showing the velocity components u , v , and w relative to the probe. Initially, a probe fitted with hot-film sensors (TSI-60) was purchased since sturdy sensors were desired for the measurements to be made on the highway. As described below, the hot-film sensors were inadequate for accurate measurements of large amplitude velocity fluctuations. Hot-wire sensors (TSI T-1.5) which proved to be adequate for the measurements, are shown mounted on the prongs of the probe and are numbered from 1 to 3. The probe was slightly modified, as discussed in section (III A), to provide a larger spacing between the sensors.

II. RESULTS FOR CALIBRATION OF PROBE FITTED WITH HOT-FILM SENSORS

A standard TSI model 1298 probe fitted with hot-film sensors (TSI-60) was mounted on the servo positioner and exposed to a uniform flow of 19.4 m/sec, comparable to the maximum speed to be used for measurements on an expressway. Linearized signals from the hot-film sensors and the signals from the servo pitch and yaw potentiometers were recorded when the probe was pitched with zero yaw and yawed with zero pitch. It was observed that the traces of the sensor outputs, plotted on an x-y plotter as functions of pitch and yaw, see Fig. 3 and 4, were irregular. The trace from sensor (2) when the probe was pitched at zero yaw and from sensor (3) when the probe was yawed at zero pitch exhibit the greatest irregularity. There is a sudden increase in the linearized output voltage as the pitch or yaw angle increases.

At first it was thought that these irregularities were

caused by non uniform flow in the wind tunnel. However, further examination of the sensor signals at discrete angles of pitch and yaw revealed that they were not constant and contained sinusoidal oscillations at various frequencies from 2 to 7 KHz. These oscillations appeared, changed and disappeared at various angles of pitch and yaw. The Reynolds number was approximately 218 based on the sensor diameter and the average component of the 19.4 m/sec. velocity normal to the slanted sensors. It is apparent that the rate of heat transfer from the sensor is not a predictable function of the angle between the axis of the sensor and the free stream velocity. It was concluded that the 152 μ m diameter hot-film sensors (TSI-60) were not suitable for use on the three sensor probe at a Reynolds number of 218.

Similar tests were then made at the same flow speed using smaller, 50.8 μ m, diameter hot-film sensors (TSI-20). The Reynolds number based on the average velocity normal to the sensors was 72.7. The variation of the sensor signal with yaw angle was found to be more regular than the signal from the 152 μ m diameter sensors; but sinusoidal oscillations of the sensor output at 5.71 and 6.11 KHz were observed at small yaw angles. Even smaller, 25.4 μ m, diameter hot-film sensors (TSI-10) were then installed and the probe was again tested at a Reynolds number based on the average normal velocity of 36.3. The sensor outputs as a function of pitch and yaw angle were much more regular than the 152 μ m diameter sensors, but 6 KHz oscillations of the sensor output and jumps in the mean signal from one of the sensors were observed at large pitch angles.

It was concluded that at this flow speed, the Reynolds numbers of the sensors were too large to allow steady, predictable rates of heat transfer. The aspect ratio of the hot-film sensors is not large (of the order of 15) and this, as well as the relatively large Reynolds number, probably contributes to the irregularity of the sensor outputs when the probe is pitched or yawed. It should also be noted that Ho¹³ has reported that electrical cross-talk occurs between the sensors on a split film probe with diameter of $152\ \mu\text{m}$. The present finding of anomalous steady and unsteady signals resulting from a change in the angle between the flow direction and the sensor axis represents an additional source of aerodynamic cross talk that may occur with split film sensors at the Reynolds numbers reported above.

III. CALIBRATION OF A MODIFIED PROBE FITTED WITH HOT-WIRE SENSORS

A. Modifications of the Probe

The TSI 1298 probe was slightly modified by spreading each of the three pairs of hot-wire prongs further apart (in a direction outward from the axis of the probe), as shown in Fig. 2, to reduce wire/prong interference at large pitch and yaw angles. The approximate diameter of a circle which would surround the wires at this larger spacing was 7 mm. Thus, turbulent velocity fluctuations with a spatial scale less than a centimeter cannot be correctly resolved by the modified probe. The modified probe was returned to the manufacturer and fitted with $3.81\text{ }\mu\text{m}$ diameter tungsten hot-wires (TSI T-1.5) with a platinum coating, a sensitive length of $1270\text{ }\mu\text{m}$ and a length to diameter ratio 333.3.

B. Determination of Probe Geometry and Calibration Constants

The probe was tested in the wind tunnel and the sensor signals were recorded in the same manner as discussed for the hot-film probes of Section II. The linearized hot-wire signals plotted as functions of pitch and yaw angle in Figs. 5 and 6, were much more regular than similar traces of the hot-film sensor outputs, see Figs. 3 and 4. The signal from sensor (2) as a function of varying pitch angle, in Fig. 5, is similar to the signal from sensor (3) as a function of yaw angle, in Fig. 6, as should be observed. Further examination of the tape recorded data using computer generated plots of the linearized output

voltage for each hot-wire revealed that the output voltage was proportional (within a few percent) to the velocity component normal to the hot-wires (the classic cosine law). The output from each sensor was assumed to obey the cosine law so that each hot-wire measures the component of the velocity normal to the wire. For three sensor probes fitted with lower aspect ratio sensors, which do not obey the cosine law, Paulsen⁷ and also Chang and Adrian⁸ used the Jorgensen⁹ cooling law to relate the sensor output to the flow velocity components.

Using the geometrical arrangement of the hot-wires shown in Fig. 2, The equations for the velocity components, U_i , normal to the i^{th} hot-wire in terms of the velocity components relative to the probe are,

$$U_1 = (u^2 + v^2)^{1/2} \quad (4)$$

$$U_2 = [(u \sin \varphi - v \cos \varphi)^2 + w^2]^{1/2} \quad (5)$$

$$U_3 = [(u \sin \Theta - w \cos \Theta)^2 + v^2]^{1/2} \quad (6)$$

where, φ , is the angle between sensor (2) and the probe axis, Θ , is the angle between sensor (3) and the probe axis and u , v and w are the velocity components parallel and normal to the probe axis as defined in Fig. 1.

The linearized output voltage, V_i , from the i^{th} hot-wire, is proportional to the velocity normal to the hot-wire, i.e.:

$$V_i = K_i U_i, \quad (7)$$

where, K_i , are constants.

The constants, K_i , determined from the digitized records of the linearized outputs for the probe, when pitched at zero yaw or yawed at zero pitch, were computed by noting the maximum output voltage for each wire occurring when the wire was normal to the flow. Close examination of the digitized data revealed that the flow in the tunnel was not exactly uniform and the probe geometry was not exact. Hot-wires (2) and (3) did not appear to be mounted accurately at 45 degrees to the probe axis or else the potentiometers used to determine the angles, Θ_p , and, Θ_y , were not correctly oriented on the servo shafts.

An iterative procedure was developed to accurately determine the effective probe geometry and alignment of the probe axis with the flow. Eqs. (1-3) were used to calculate the velocity components, u , v , and w as functions of pitch and yaw angles, Θ_p , and Θ_y . Then Eqs. (4-6) were used to compute the velocities normal to each wire. The calculated values of velocity normal to each wire must agree with the measured values given by Eq. (7) using the previously determined constants, K_i . The above calculations were performed using various assumed values for the probe geometry (the angles, ϕ , and Θ) and for various assumed values of the initial alignment of the probe axis with respect to the tunnel axis. The best correspondence between the calculated and measured normal velocity components,

for each wire, was obtained with the probe geometry, $\Theta = 38$ degrees and, $\phi = 45$ degrees. The probe yaw axis alignment angle, Θ_y , was found to be correct, but the pitch axis alignment angle, Θ_p , was discovered to be 5 degrees larger than indicated by the servo pitch axis potentiometer. The above values for the probe geometry and alignment of the probe axis with the flow were used in the remainder of the paper.

During the above procedure, the response of sensor (1), when the probe was pitched at zero yaw angle, indicated that the mean tunnel speed in the vertical plane of the test section was uniform in the upper part of the test section (for pitch angles, $\Theta_p > 0^\circ$), but the speed was higher in the lower half (for a pitch angle, $\Theta_p = -50^\circ$ the speed was 5% greater than on the centerline). It is possible that the flow speed varies by 5% at other locations in the test section, but further measurements of the flow uniformity were not performed. For this reason, the probe calibration is not as accurate as it would have been in a more uniform flow and the measured velocity components described below may be in error by 5%.

IV. SIMPLIFICATION OF THE THREE SENSOR PROBE EQUATIONS

Eqs. (4-7) must be solved for u , v , and, w when the three linearized voltages, V_i , are measured. From Eqs. (7) and the calibration constants, K_i , the velocity components normal to each sensor, U_i , are known. The velocity components, u , v , and, w , must then be found from Eqs. (4-6). Numerical methods were used to solve these simultaneous algebraic equations.

The equations have multiple roots. The response of each hot-wire depends upon the magnitude of the normal velocity and remains the same when the velocity is reversed. The existence of multiple roots, but not the number of roots, is well known and has been discussed by many investigators including Paulsen⁷ and Chang, Adrian and Jones⁸. Recently, Willmarth¹⁴ presented a geometric interpretation for velocity measurements made with three-sensor probes which shows that, in general, there are eight possible velocity vectors that can produce a single set of three normal velocity signals.

In their paper, Chang, Adrian and Jones⁸ used the criterion that the correct velocity vector among the multiple results is the one with the least angle from the mean flow direction. They found this to be valid for low intensity turbulence, but for highly turbulent flows the wrong result was obtained. The problem has not been resolved, in fact Chang, Adrian, and Jones⁸ state that, "the selection of the right velocity vector among the multiple results becomes a major task for the three dimensional velocity measurement in higher intensity turbulent flow". It was decided that the best solution possible would be obtained in the present work and since the correct solution is known, from the probe orientation, the limits of validity of the solution could be determined. The problem of verifying the correctness of the solution in a turbulent flow when the correct solution is unknown (as in the measurements cited by Chang, Adrian and Jones⁸) is left for future studies.

In order to solve Eqs. (4-6) for each set of the three values of U_i , Eq. (4) was first solved for positive values of u only,

$$u = [U_1^2 - v^2]^{1/2}, \quad (8)$$

(which eliminates reversed flow solutions along the probe axis), and substituted into Eq. (6) to give an expression for w , in terms of u , and v ,

$$w = u \tan \Theta - [U_3^2 - v^2]^{1/2} \sec \Theta. \quad (9)$$

The sign of the radical in Eq. (9) was again chosen (in agreement with the choice of sign in Eq. 8) to eliminate reversed flow along the probe axis, $u < 0$, when, w , and, v , are zero or small compared to, U_3 . Eqs. (8) and (9) were substituted into Eq. (5) to obtain an expression, depending only on v :

$$F(v) = [(U_1^2 - v^2)^{1/2} \sin \varphi - v \cos \varphi]^2 + [(U_1^2 - v^2)^{1/2} \tan \Theta - (U_3^2 - v^2)^{1/2} \sec \Theta]^2 - U_2^2 = 0. \quad (10)$$

When Eq. (10) is solved for, v , the components, u , and, w , are found from Eqs. (8) and (9).

V. ITERATIVE SOLUTION OF THREE SENSOR PROBE EQUATIONS

Newton's method of iterative solution was used to find the zeros of Eq. (10). For an initial value of v , say v_0 , $F(v_0)$ and $dF(v_0)/dv$ are used to find a better approximation of v , v_{new} :

$$v_{\text{new}} = v_0 - F/(dF/dv). \quad (11)$$

By differentiating Eq. (10) find,

$$(dF/dv)/(2u) = G[v/u, (U_1^2 - v^2)/(U_3^2 - v^2)] \quad (12)$$

where the equation has been written in dimensionless form and,

$$G(x,y) = x[1 - 2\sin^2\varphi - (1+\sin^2\Theta)/\cos^2\Theta] \\ + x(\tan\Theta/\cos\Theta)(y + 1/y) + (x^2 - 1)\sin\varphi \cos\varphi, \quad (13)$$

with: $x = v/u$ and $y = [(U_3^2 - v^2)/(U_1^2 - v^2)]^{1/2}$.

A) Stability of the iterative solution

Newton's method is unstable when $dF(v)/dv = 0$, i.e. $G(x,y) = 0$. The points $(w/u, v/u)$ for which $G(x,y) = 0$ were found numerically. Since $G(x,y) = 0$ is quadratic in, y , for any value of, x , the two roots for y were computed numerically for many values of, $x = v/u$. Then for each root, y , the corresponding value of w/u , was computed from Eq. (6), rewritten (with the aid of Eq. (4)) as,

$$w/u = \tan\Theta - y \sec\Theta \quad (14)$$

For each value of v/u , there are two values of w/u , for which $dF/dv = 0$. The points $(w/u, v/u)$ for which $dF/dv = 0$ were computed for the probe geometry, $\Theta = 38^\circ$, and $\varphi = 45^\circ$, and plotted in Fig. (7).

VI. NUMERICAL TEST OF THE ITERATIVE SOLUTION

Two FORTRAN programs were written to test the performance of the probe when exposed to different variations of the flow velocity. Numerical data for the normal velocities was generated by substituting known values of u , v , and w into Eqs. (4-6). These data are guaranteed to be correct, unlike experimental data which are always subject to error. The peculiarities of the probe geometry and the iteration procedure can best be examined using numerical data.

Both programs first calculated the velocity components u , v , and, w using Eqs. (1-3), then the velocity normal to each hot-wire, using Eqs. (4-6), and finally performed an iteration procedure to calculate u , v , and w from the normal velocities. Each iteration was carried out to an accuracy in v of .01 ft/sec, (approximately 0.02% of the stream velocity). The starting value for v in each iteration was the previous value of v obtained in the previous iteration. This was done to increase the stability of the Newton iteration procedure and reduce the number of steps in each iteration.

The first test program alternately incremented and/or decremented the pitch and yaw angles in one degree steps creating a "path" in the pitch-yaw plane which was a rectangular "spiral" emanating from the outward from the origin. The spiral continued outward until the pitch and yaw angles reached 60 degrees. The initial starting value of the first iteration was $v = 0$. If the iteration failed (negative arguments in the radicals or non-convergence) the iteration was restarted at the next point on

the spiral with the initial guess for the value of v being the correct value of v .

The u , v , and w solutions found by iteration were processed to eliminate solutions which grossly disagreed with the correct values. Fig. 8 shows those values of v/u and w/u corresponding to iterative solutions of u , v , and w which agree with the correct values to within 5.0 ft/sec. Interesting features of the figure include the two triangular shaped holes in the first and third quadrants of the plots, and the dark band of points along the curved upper limit of the fourth quadrant.

For values of v/u and w/u less than 0.35 the iteration procedure was reliable and the resulting solutions were quite accurate. For most turbulence measurements, when the turbulent intensity is not too large, these results are more than adequate.

Closer examination of Fig. 8 for larger values of v/u and/or w/u revealed that the upper slanted edge of the hole in the first quadrant, the lower slanted edge of the hole in the third quadrant, and the curve across the top of the plot in the fourth quadrant are all segments of the boundary, $dF(v)/dv = 0$ shown in Fig. 7. The holes in the first and third quadrant were formed when the path followed during variation of the pitch and yaw angles approached the boundary from the side opposite the origin and the solution "reflected" off the boundary in the direction of the incorrect solution and later failed. The dark band across the top of the plot in the fourth quadrant was formed when the solution path approached the boundary from the side nearest the

origin and reflected back toward the origin. In these cases, the solution continued quite some time before failing. Since the correct solution was known in this test it was possible to identify the errors, but it would be very difficult to determine the correctness of the solution under actual conditions when measuring time resolved velocity components of large amplitude.

A more demanding test of the iteration procedure was made in the second FORTRAN test program. The "path" in the pitch-yaw plane began at the point where the pitch and yaw angles are -60 degrees. The pitch angle was incremented in one degree steps until it reached 60 degrees. Then the yaw angle was increased one degree and the pitch angle was again varied from -60 to 60 degrees. In contrast to the first program, if the iteration failed, the pitch angle was increased by one degree and the iteration procedure was restarted with an initial guess for v of zero.

Fig. 9 is a plot of the values of v/u and w/u generated by the second test program which were within 5.0 ft/sec of the correct values. Again, it should be noted that the iteration scheme performs quite well in the vicinity of the origin. As expected, most of the good points lie inside the boundary. The use of the initial guess, $v = 0$, when restarting the iteration after failure was an attempt to insure that the solution on the side of the boundary nearest the origin will be obtained. This is a realistic test of the iteration procedure since when making actual measurements one will not know the correct solution or where it is located relative to the boundary.

The second test is a more demanding test of the iteration procedure. The use of the previous value of v as the initial guess for the next step in the iteration procedure is severely tested when the pitch angle jumps from 60 to -60 degrees. When restarting the procedure with the initial guess of $v = 0$, the iteration procedure was observed to converge to solutions lying on the side of the boundary $dF(v)/dv = 0$ adjacent to the origin. A comparison of Figs. 8 and 9 reveals that the holes in the plots do not coincide. This indicates the sensitivity of the iteration to the starting values and to the "path" relative to the boundary. A test was made in which the iteration procedure was started at the origin and the yaw angle was varied from zero to negative values in one degree steps. The correct solution was then found along the $v/u = 0$ axis in the region of the hole in Fig. 9. Apparently, the iteration procedure is unstable and/or sensitive to the value used to begin the procedure in this region.

VII. ITERATIVE SOLUTION FOR MEASURED DATA

The iteration process was performed using hot-wire signals measured when the probe was manually pitched and yawed at random for a constant free stream velocity. When the iteration did not converge or the argument of one of the radicals in Eq. 10 became negative the iteration was restarted again at the next data point with an initial value of $v = 0$. The probe pitch and yaw angles and the three hot-wire signals were recorded on analog magnetic tape and digitized off line. The pitch and yaw angles for this data were often very large, greater than 45° , and in this case the iterative solution frequently failed to give a solution or gave erroneous results.

Figs. (10-12) show the velocity components computed by iteration compared to the actual velocity components computed from Eqs. (1-3). The data shown in Figs. (10-12) have been screened, using the computer, to eliminate solutions for which any velocity component differs by more than 5 ft./sec. from the correct velocity component computed from the probe pitch and yaw angles, see Eqs. (1-3). The data of Figs. (10-12) show that the probe is capable of measuring velocity components produced by flow at large angles to the probe axis with reasonable accuracy, but it is essential that one have additional data to reject incorrect solutions.

Another test of the accuracy of the iterative solution was made by comparison of the iteratively computed and the actual time resolved velocity component data when the probe was randomly pitched and yawed for moderate angles. The traces shown in Fig.

(13) are the actual and the iteratively computed velocity components during random pitch and yaw of the probe at a wind tunnel speed of approximately 65 ft./sec. The velocity traces have been plotted so that the origin for the computed velocity components is 5 ft./sec. greater than the origin for the actual velocity components. The iterative solution for v/u and, w/u , is also shown in Fig. 14. The data of Fig. 14 do not reach the boundary, shown in Fig. 7, where $dF(v)/dv = 0$ and there were no failures of the iteration procedure for this data. However, some of the data are incorrect.

The incorrect data, for which the computed and true velocity components differ by more than 5 ft./sec., have been replotted and flagged (by setting the iteratively computed velocity components to zero) and are plotted in Fig. 15 with the origin of the correct velocity traces 5 ft./sec. above the computed velocity traces. The streamwise velocity component, u , was fairly accurate, but the cross stream velocity components were in error at large amplitudes. The most serious error occurred at the midpoint of the data where the true and computed, v and w , traces cross over each other. The cause of the errors are discussed in the next section.

VIII. DISCUSSION AND CONCLUSIONS

When the probe was calibrated for this investigation, it was found that the stream velocity in the test section of the tunnel was 5% greater in the lower portion of the test section than in the upper half. This was not deemed significant for the measurements shown in Fig. 13 and 15 because the pitch and yaw angles of the probe were sufficiently small that the sensors remained near the center of the tunnel. The near equality of the measured and correct velocity traces for, u , shown in Fig. 13 and 15 support this conclusion.

However, the accuracy is not as good for velocity components transverse to the probe axis. When either, v/u , or, w/u , were of the order of 0.25, or greater, a large number of errors were found for positive values of, v , or, w . Some errors were also found for negative values of, v , near the left side of Fig. 15 and for small values of, v , near the center of the trace shown in Fig. 15. There appear to be three primary reasons for these errors.

1. Instability of the Method of Iterative Solution

The instability of the Newton method when $dF(v)/dv = 0$ is a serious source of error. Tests of the method, see Sec. IV, showed that the iteration placed more points near the curves where $dF(v)/dv = 0$, Fig. 8 and 9, (hereafter termed the boundary) than elsewhere on the plot. However, a similar plot, including only points where the iteration agreed with the correct data to within 0.5 ft./sec., showed the data distribution to be

uniform all the way to the boundary. The extra data along the boundaries in Fig. 8 and 9 were found to correspond to values of v/u and w/u originally lying on the other side of the boundaries. This shows that even when the velocity components normal to the sensors are correct, the iteration procedure often found the incorrect solution. Observe that the boundary is relatively close to the origin in the first quadrant of the $w/u, v/u$ plane, passing through the point, $v/u = w/u = 0.38$. This may be why most of the errors in the v traces and all of the errors in the w traces of Fig. 15 occur for positive values of v and w .

The iteration procedure is also sensitive to the initial starting value of v . The test in Section VI could not find solutions in the blank part of the third quadrant of Fig. 8., but the correct solution was found when the iteration was started at the origin, $v = w = 0$. The erroneous data for negative, v , in the trace at the left hand side of Fig. 15 may have been caused by an instability of this type.

It is concluded that improved accuracy of the solution is possible if one can find better iteration procedures and/or methods for restarting the procedure when it fails to converge. With adequate iteration procedures a three sensor probe can be used for time resolved measurements of three velocity components in a turbulent flow if the turbulence level is not too large.

2) Incorrect Measurement of the Velocity Normal to the Sensors

For certain sets of velocity components normal to the sensors which correspond to points $(w/u, v/u)$ near the boundary there may be no real solution for Eq. (10), if one or more of the velocity components normal to the sensor is erroneous. Errors in measurement of the velocity normal to the sensors can be caused by errors in electrical measurement, aerodynamic prong interference, flow nonuniformity with a scale less than the sensor spacing, poor sensor calibration, dirt on a sensor and sensor vibration, see Perry³.

3) Multiple Solutions of Eqs. (4-6)

The existence of multiple solutions for a given set of values of velocity components normal to the sensors can result in unavoidable and unrecognizable errors in the solution of Eqs. (4-6). Using a geometric interpretation for measurements made with multiple sensor probes, Willmarth¹⁴ found that there are, in general, eight velocity vectors which can cause a single set of three velocity components normal to the sensors. Four of these solutions, with $u < 0$, have been eliminated from consideration. By using the geometric interpretation one can verify that there are always two possible velocity vectors when the transverse velocity components are small. One vector is correct and the other is an incorrect vector at a large angle with respect to the probe axis. One can then choose the solution with the least transverse velocity. Chang, Adrian, and Jones⁸

recognized this for their probe configuration and chose the solution with a flow direction making the least angle with the probe axis.

When the transverse velocity is larger, there are either two or four possible solutions, with $u > 0$, as can be shown using the above cited geometric interpretation for a particular three sensor probe, and only one solution is correct. In this case there is no way to determine the correct solution of Eqs. (4-6) without additional information, beyond that obtained from measurements made with three sensors. It is suggested that one might use additional sensors to provide more information so that the correct solution can be determined. This would be an interesting problem for further investigation, but would make the measurements and data reduction more complex.

ACKNOWLEDGEMENTS

The continued support of the Office of Naval Research under contract number N00014-76-C-0571 during the course of this investigation is gratefully acknowledged.

REFERENCES

1. Comte-Bellot, G., Ann. Rev. Fl. Mech. 8, 209 (1976).
2. Blackwelder, R.F., Methods of Experimental Physics: Fluid Dynamics Edited by Emrich, R.J. 18A, 259 (1981).
3. Perry, A.E., Hot-wire Anemometry Oxford: Clarendon Press (1982)
4. Lakshminarayana, B. and Poncet, A., J. Fluids Eng. 96, 87 (1974).
5. Moffat, R.J., Yavuzkurt, S. and Crawford, E., Proceedings Dynamic Flow Conference, Edited by Hansen, B.W. (1978).
6. Fabris, G., Rev. Sci. Inst. 49, 654 (1978).
7. Paulsen, L., J. Phys. E: Sci. Instrum. 16, 554 (1983).
8. Chang, P.H., Adrian, R.J., and Jones, B.G., Eighth Biennial Symp. on Turbulence, Univ. Missouri Rolla, MO. (1983).
9. Jorgensen, F.E., Disa Information No. 11, 31 (1971).
10. Wallace, J.M., Am. Soc. Civil Engrs. Spec. Conf. 2, 1250 (1983).
11. Willmarth, W.W. and Wei, T., Bull. Am. Phys. Soc. 27, 9, SS3 (1983).
12. Uberoi, M.S., J. Aero. Sci. 23, 754 (1956)
13. Ho, Chih-Ming, Rev. Sci. Inst. 53, 1240 (1982).
14. Willmarth, W.W., Accepted, Phys. Fluids (1984).

FIGURE CAPTIONS

Fig. 1 Line drawing of servo positioner used for pitch and yaw calibration of the three sensor probe in a uniform flow in the wind tunnel. The housing of the pitch servo, (A), is fixed and the housing of the yaw servo, (B), is mounted on the rotating shaft of the pitch servo. The three sensor probe is in turn mounted on the rotating shaft of the yaw servo but the three sensors at the head of the probe are not shown. The velocity components with respect to the probe are $(u, v, \text{ and } w)$ as shown in the sketch.

Fig. 2 Sketch of Modified TSI Type 1298 Three Sensor Probe Fitted with Hot-Wires (TSI model T1.5). The velocity components normal to each sensor are: $U_1 = (u^2 + v^2)^{1/2}$,
 $U_2 = [(u \sin \varphi - v \cos \varphi)^2 + w^2]^{1/2}$, and
 $U_3 = [(u \sin \Theta - w \cos \Theta)^2 + v^2]^{1/2}$

Fig. 3 Response of sensors to pitch at zero yaw, TSI 1298 probe fitted with hot-film sensors, (TSI-60). Sensor diameter = 0.152 mm, length = 2.032 mm. $Re_d = 218$.

Fig. 4 Response of sensors to yaw at zero pitch, TSI 1298 probe fitted with hot-film sensors, (TSI-60). Sensor diameter = 0.152 mm, length = 2.032 mm. $Re_d = 218$.

- Fig. 5 Response of sensors to pitch at zero yaw. Modified TSI 1298 probe fitted with hot-wire sensors, (TSI T1.5). Sensor diameter = 0.0038 mm, length = 1.27 mm. $Re_d = 5$.
- Fig. 6 Response of sensors to yaw at zero pitch. Modified TSI 1298 probe fitted with hot-wire sensors, (TSI T1.5). Sensor diameter = 0.0038 mm, length = 1.27 mm. $Re_d = 5$.
- Fig. 7 Plot of values of $(w/u, v/u)$ for which $dF/dv = 0$. At these points the iteration scheme is unstable.
- Fig. 8 Results of test of the iteration procedure when performed, using synthetic data for the velocity normal to each hot-wire, along a path forming a rectangular "spiral" emanating outward from the origin. Points plotted are those for which the computed velocity components are within 5 ft/sec of the correct values.
- Fig. 9 Results of test of the iteration procedure when performed, using synthetic data for the velocity normal to each hot-wire, as the pitch angle was increased from negative to positive values at constant yaw angles. Points plotted are those for which the iteratively computed velocity components were within 5 ft/sec of the correct values.

- Fig. 10 Axial velocity component, u , computed by iteration compared to the correct value obtained from Eqs. (1-3). Pitch and yaw angles often exceeded 45° , thus only iteratively computed values within 5 ft/sec of correct values are shown. Free stream velocity = 65 ft/sec.
- Fig. 11 Same as Fig.10, for the transverse component, v .
- Fig. 12 Same as Fig.10, for the other transverse component, w .
- Fig. 13 Time resolved traces of the iteratively computed velocity components compared to the correct velocity components. Correct velocity component traces are plotted displaced 5 ft/sec above computed traces. Probe pitch and yaw angles restricted to relatively small angles. Free stream velocity approximately 65 ft/sec.
- Fig. 14 Plot of iteratively computed values of, w/u vs v/u , for data shown in Fig. 13.
- Fig. 15 Same data as shown in Fig. 13, with iteratively computed velocity component differing by more than 5 ft/sec from the correct value set to zero.

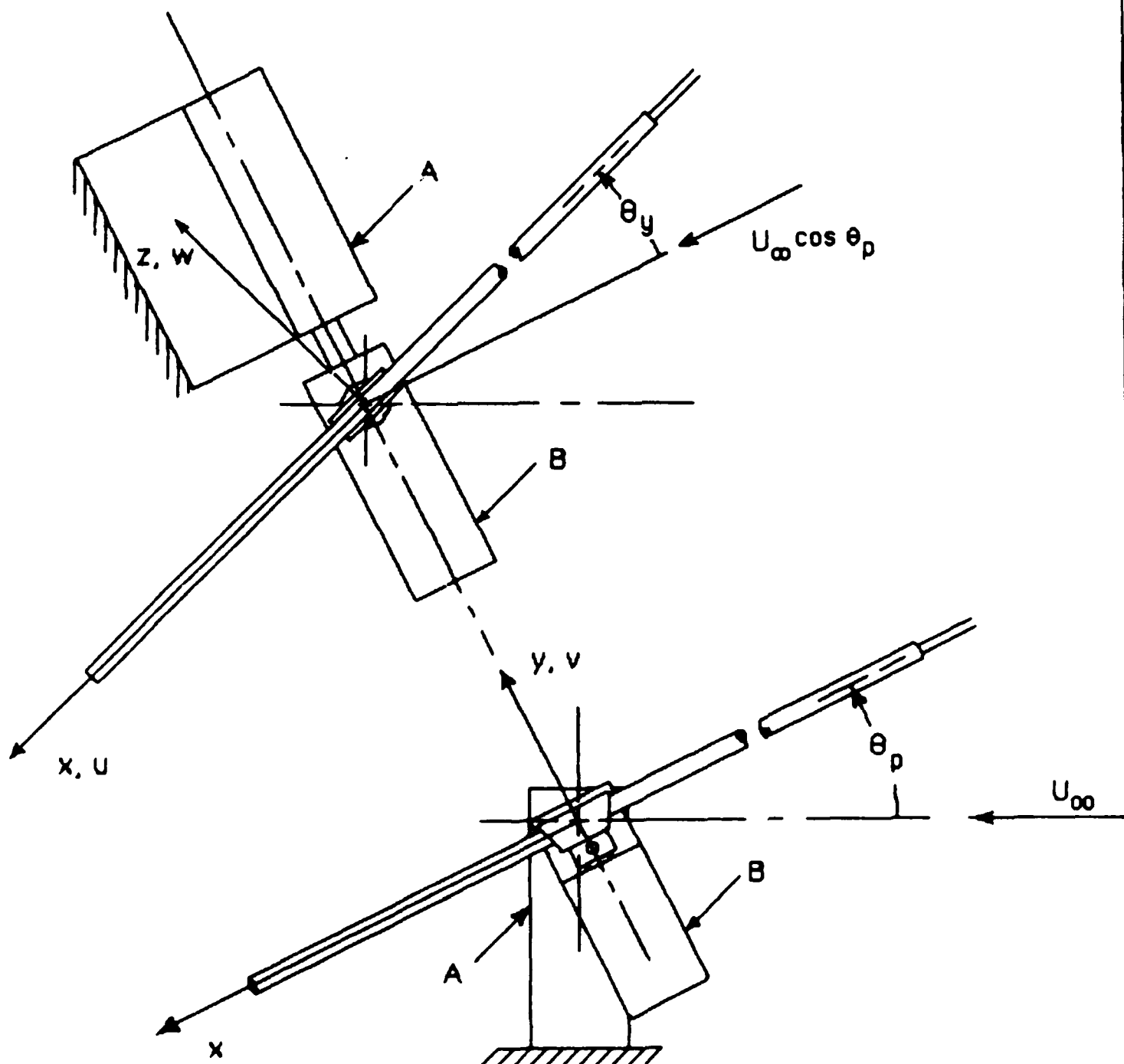


Fig. 1 Line drawing of servo positioner used for pitch and yaw calibration of the three sensor probe in a uniform flow in the wind tunnel. The housing of the pitch servo, (A), is fixed and the housing of the yaw servo, (B), is mounted on the rotating shaft of the pitch servo. The three sensor probe is in turn mounted on the rotating shaft of the yaw servo but the three sensors at the head of the probe are not shown. The velocity components with respect to the probe are (u , v , and w) as shown in the sketch.

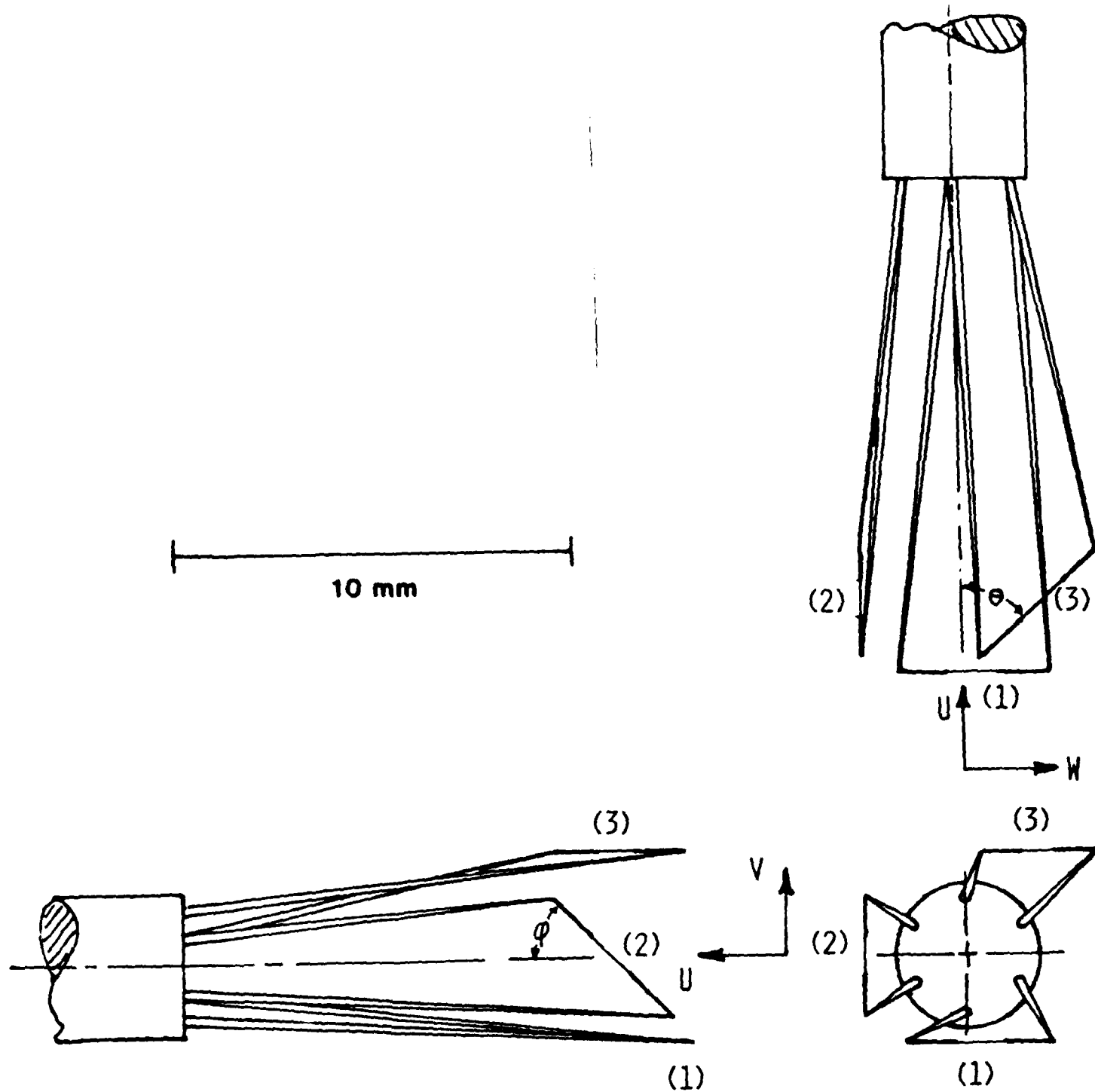


Fig. 2 Sketch of Modified TSI Type 1298 Three Sensor Probe Fitted with Hot-Wires (TSI model T1.5). The velocity components normal to each sensor are: $U_1 = (u^2 + v^2)^{1/2}$, $U_2 = [(u \sin \phi - v \cos \phi)^2 + w^2]^{1/2}$, and $U_3 = [(u \sin \theta - w \cos \theta)^2 + v^2]^{1/2}$.

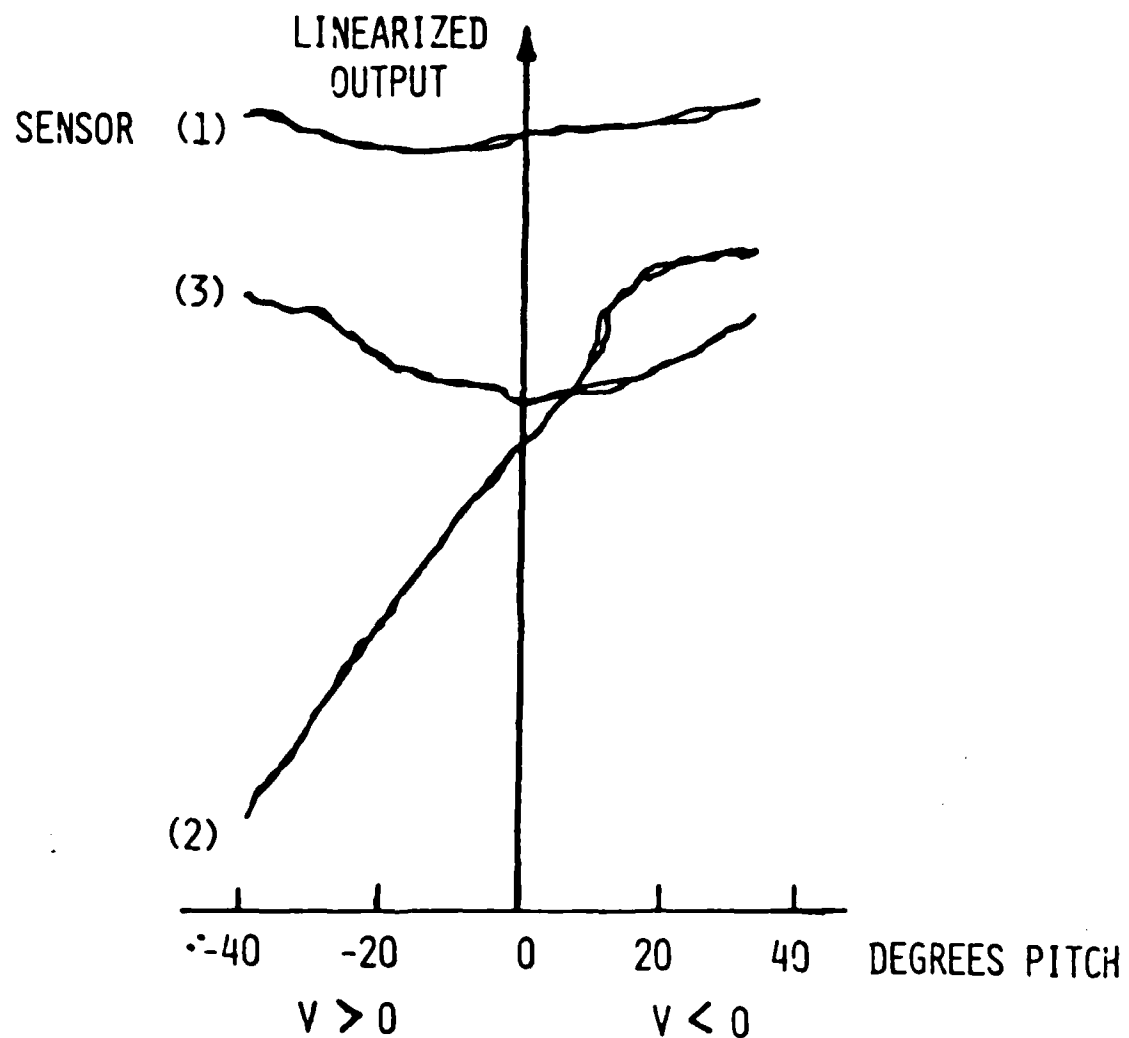


Fig. 3 Response of sensors to pitch at zero yaw, TSI 1298 probe fitted with hot-film sensors, (TSI-60). Sensor diameter = 0.152 mm, length = 2.032 mm. $Re_d = 218$.

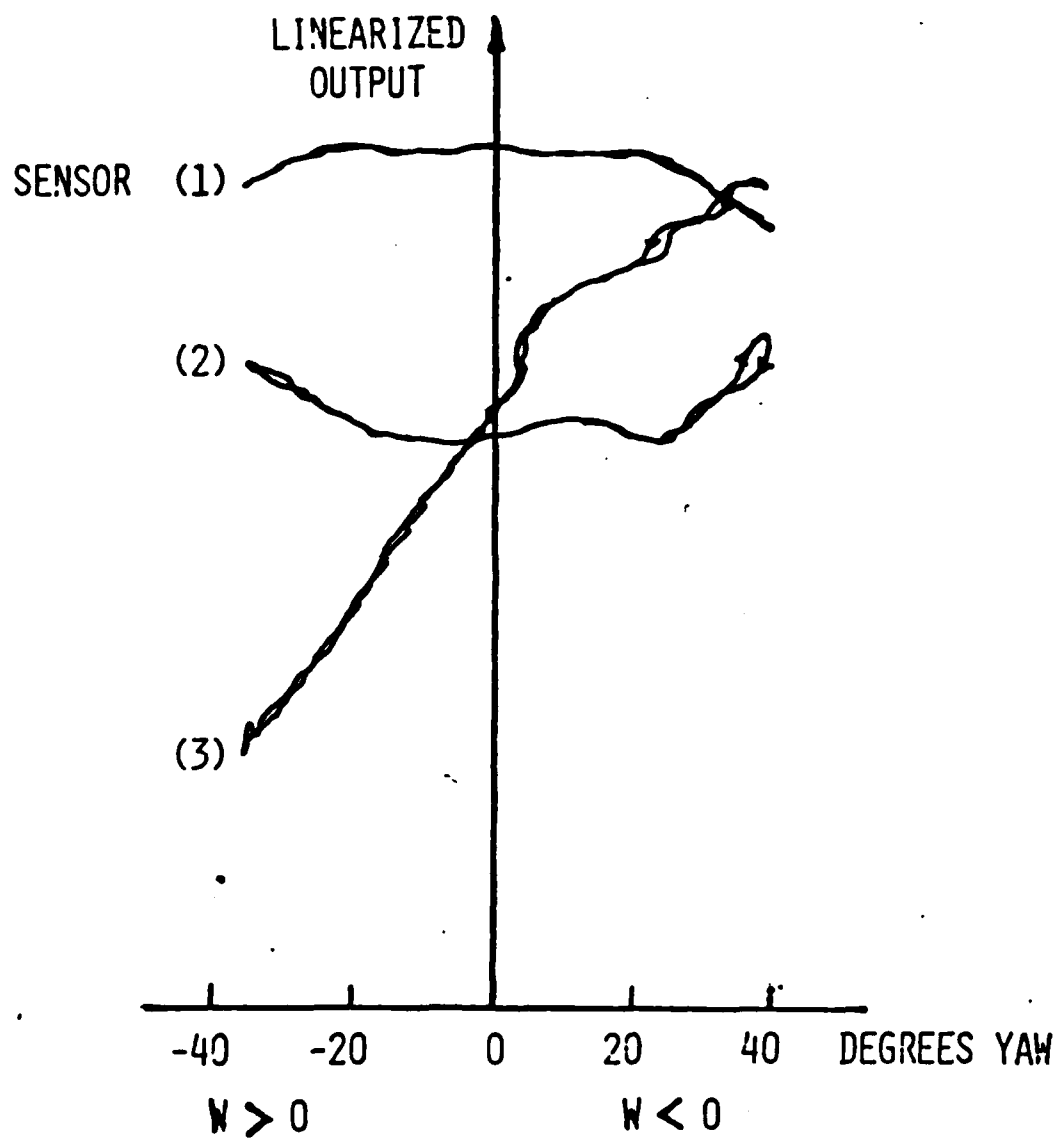


Fig. 4 Response of sensors to yaw at zero pitch, TSI 1298 probe fitted with hot-film sensors, (TSI-60). Sensor diameter = 0.152 mm, length = 2.032 mm. $Re_d = 218$.

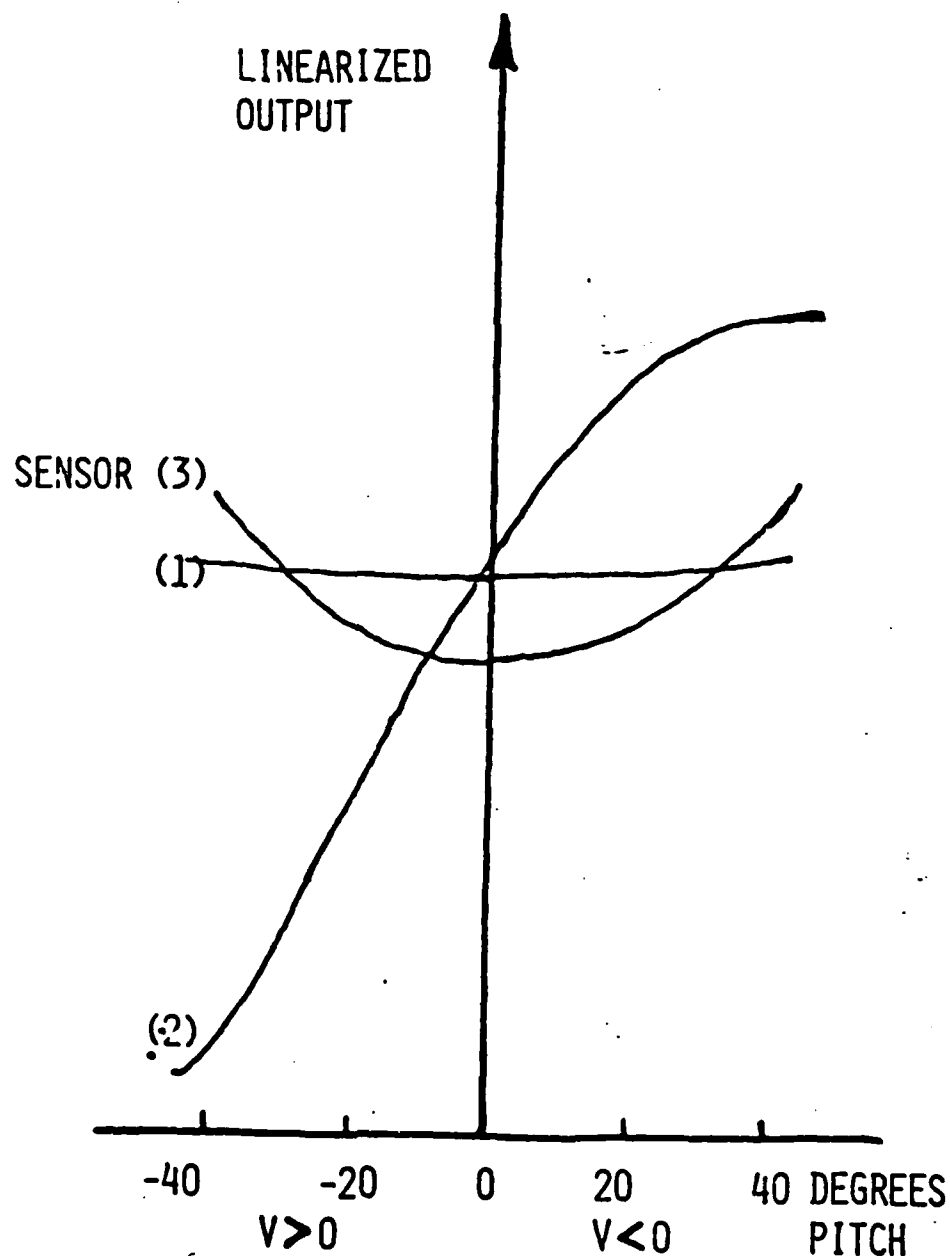


Fig. 5 Response of sensors to pitch at zero yaw. Modified TSI 1298 probe fitted with hot-wire sensors, (TSI T1.5). Sensor diameter = 0.0038 mm, length = 1.27 mm. $Re_d = 5$.

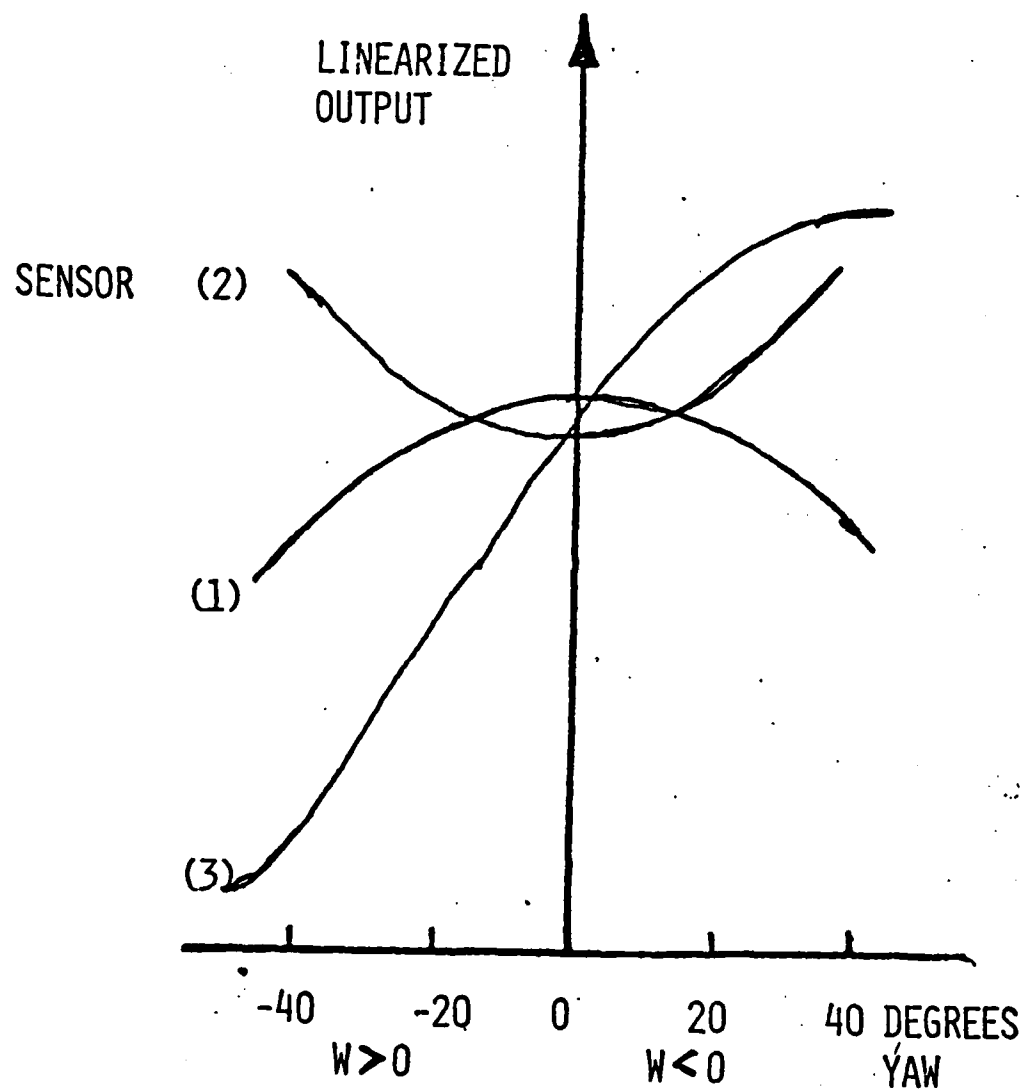


Fig. 6 Response of sensors to yaw at zero pitch. Modified TSI 1298 probe fitted with hot-wire sensors, (TSI T1.5). Sensor diameter = 0.0038 mm, length = 1.27 mm. $Re_d = 5$.

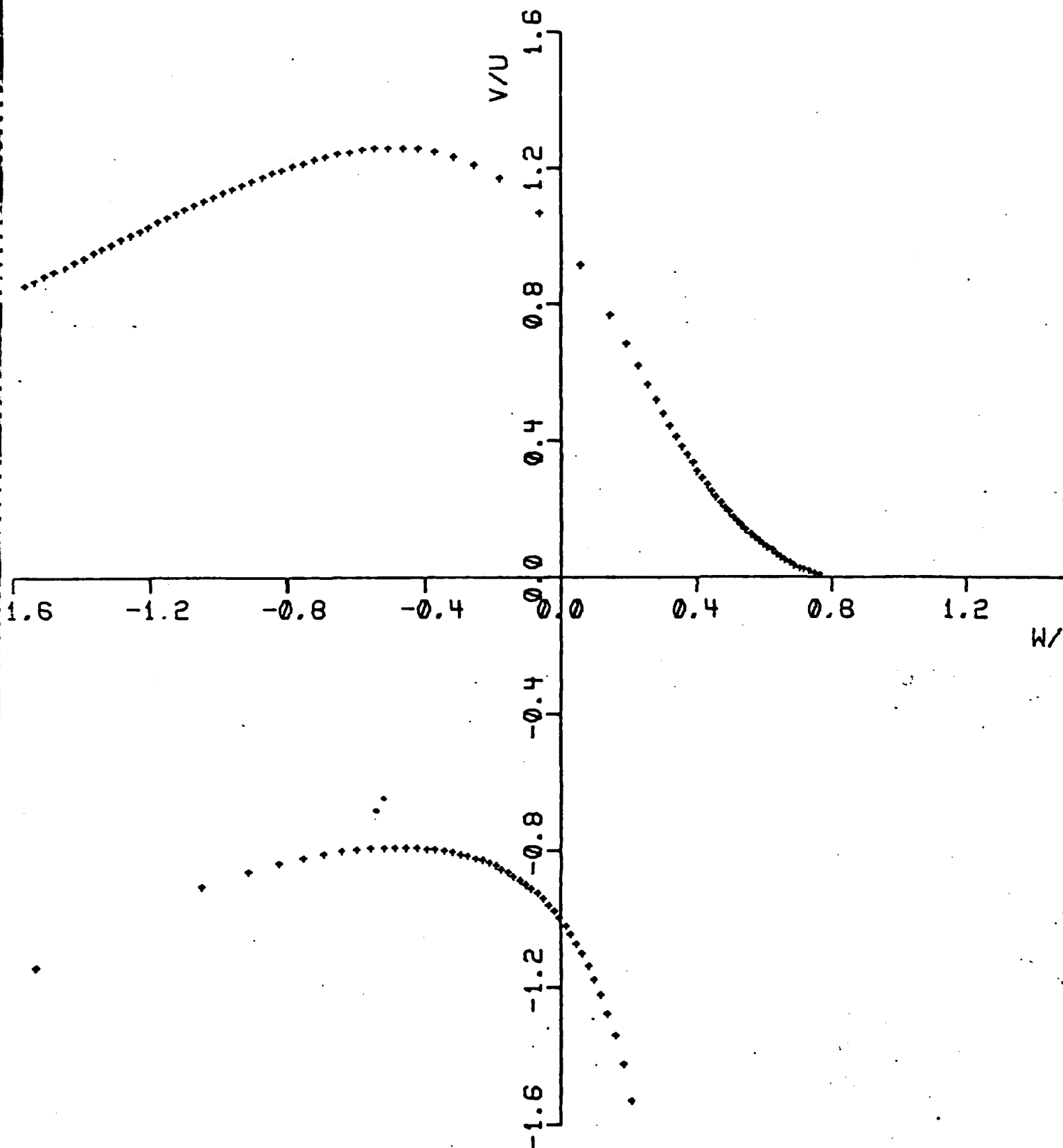


Fig. 7 Plot of values of $(w/u, v/u)$ for which $dF/dv = 0$. At these points the iteration scheme is unstable.

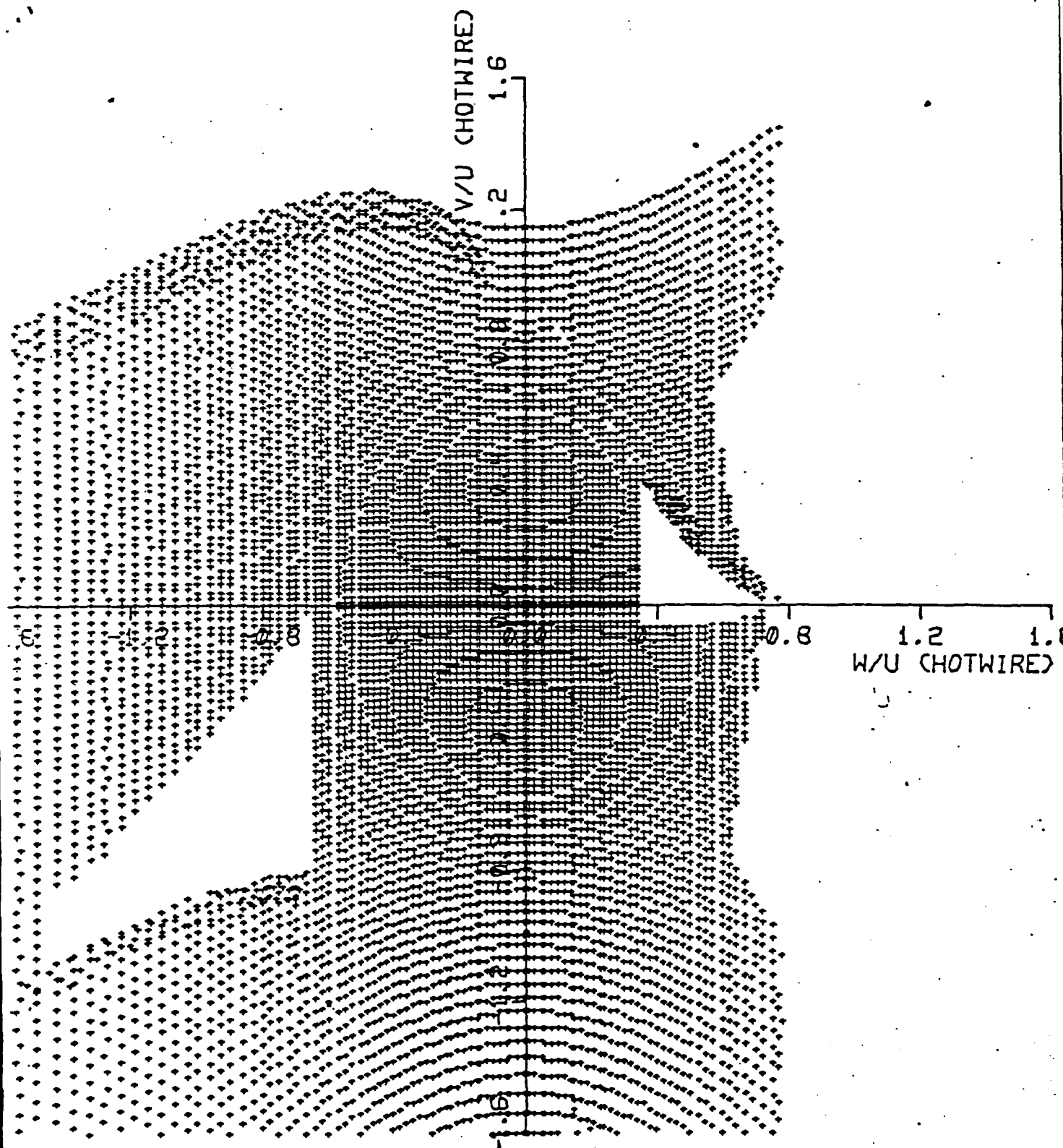


Fig. 8 Results of test of iterative solution using synthetic data generated in a rectangular spiral outward from origin. Points plotted are iteratively computed velocity components that were within 5 ft/sec of the correct values.

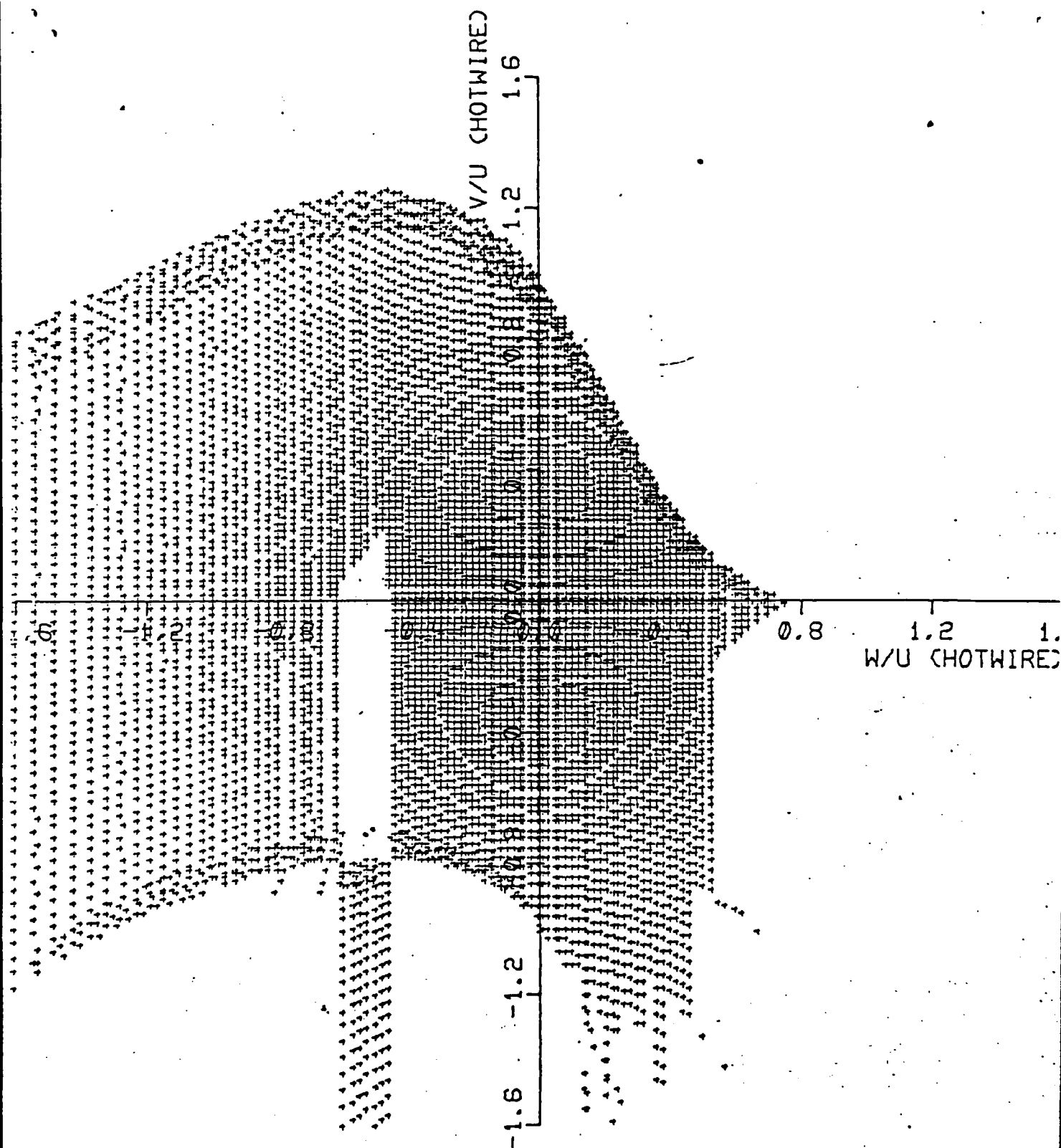


Fig. 9 Results of test of iterative solution using synthetic data generated by sweeping probe through pitch angles of -60 to plus 60 degrees at constant yaw angles. Points plotted are iteratively computed velocity components that were within 5 ft/sec of the correct values.

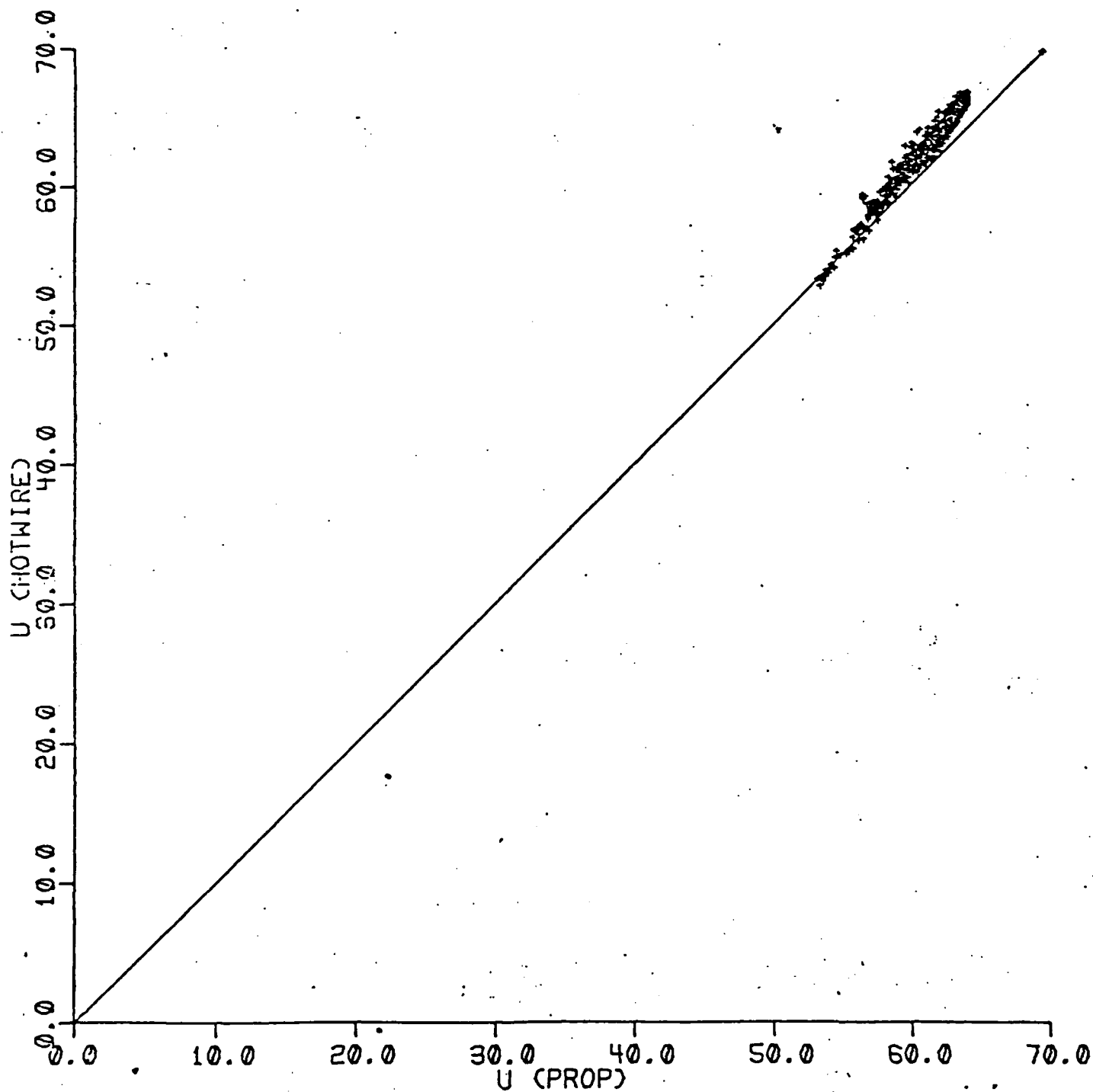


Fig. 10 Axial velocity component, u , computed by iteration compared to the correct value obtained from Eqs. (1-3). Pitch and yaw angles often exceeded 45° , thus only iteratively computed values within 5 ft/sec of correct values are shown. Free stream velocity = 65 ft/sec.

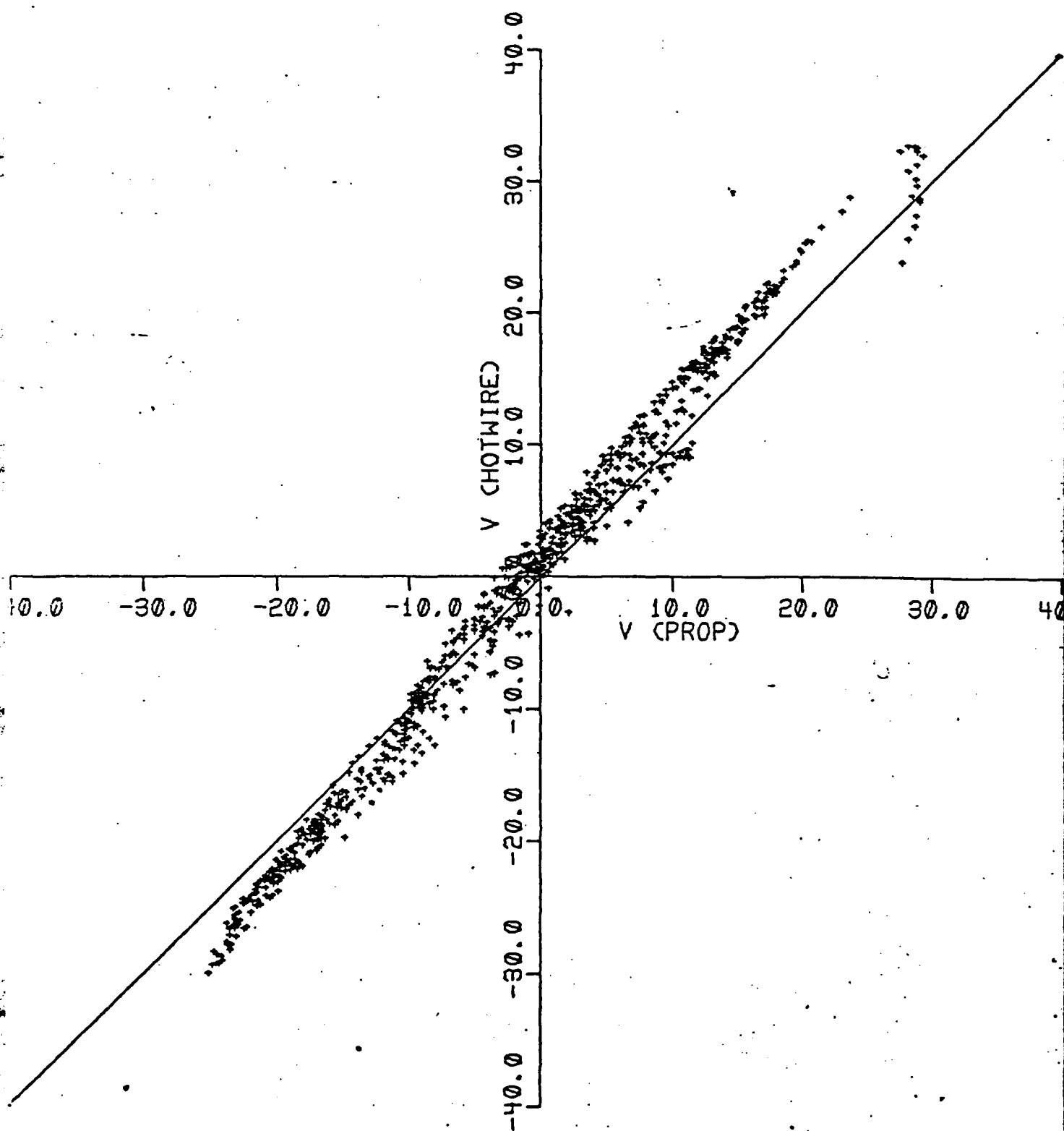


Fig. 11 Same as Fig.10, for the transverse component, v .

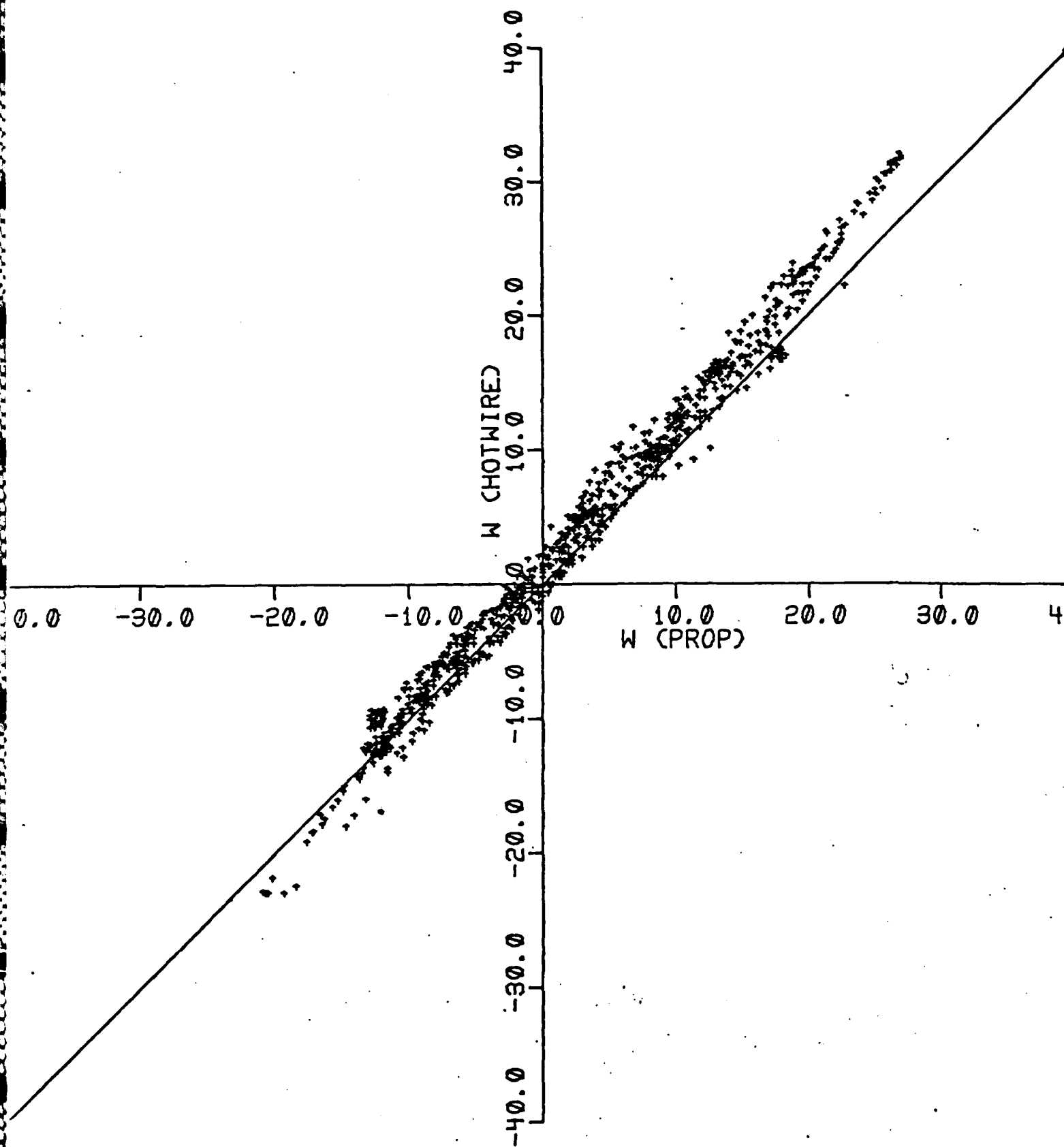


Fig. 12 Same as Fig.10, for the other transverse component, w .

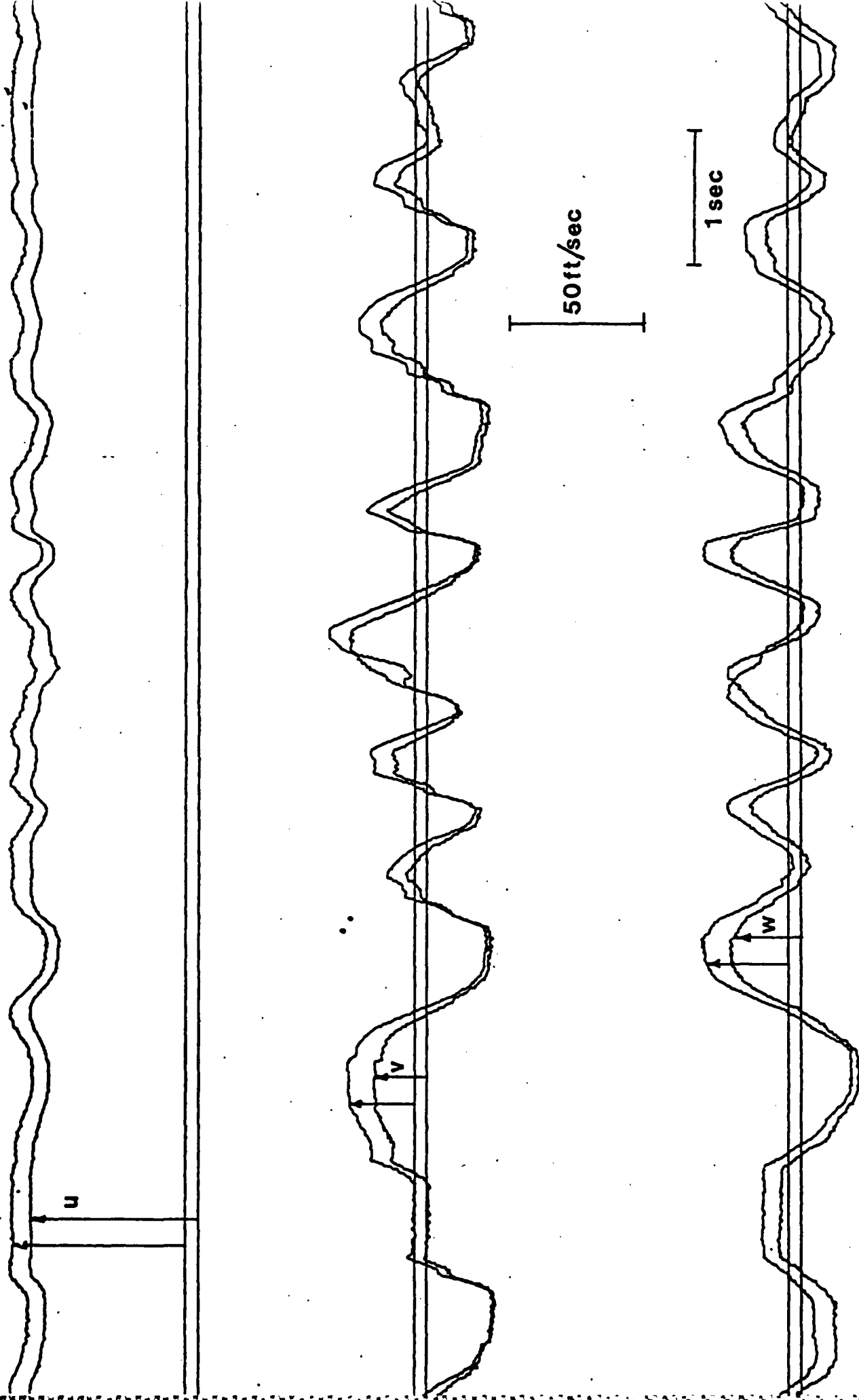


Fig. 13 Time resolved traces of the iteratively computed velocity components compared to the correct velocity components. Correct velocity component traces are plotted displaced 5 ft/sec above computed traces. Probe pitch and yaw angles restricted to relatively

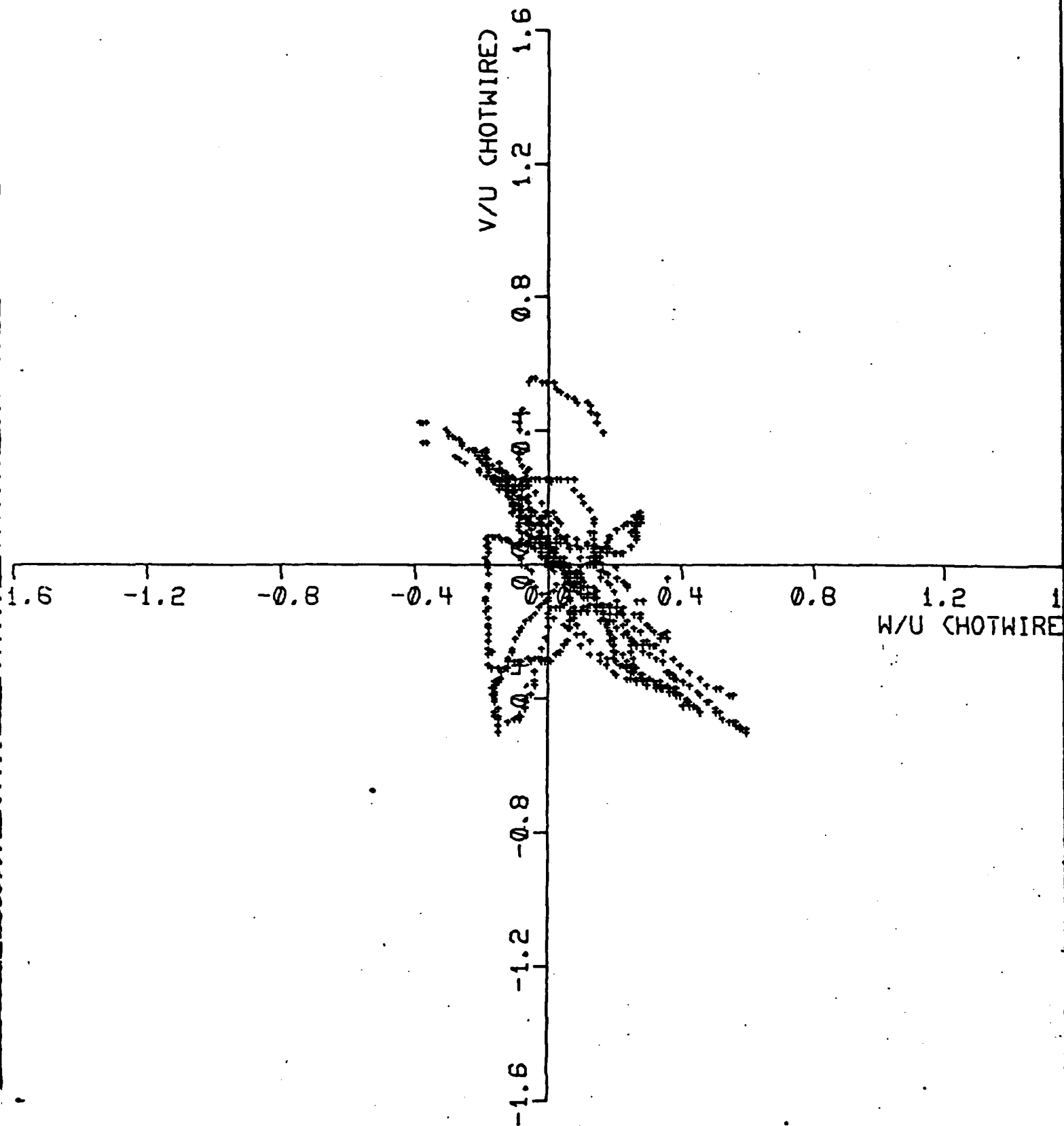


Fig. 14 Plot of iteratively computed values of, w/u vs v/u , for data shown in Fig. 13.

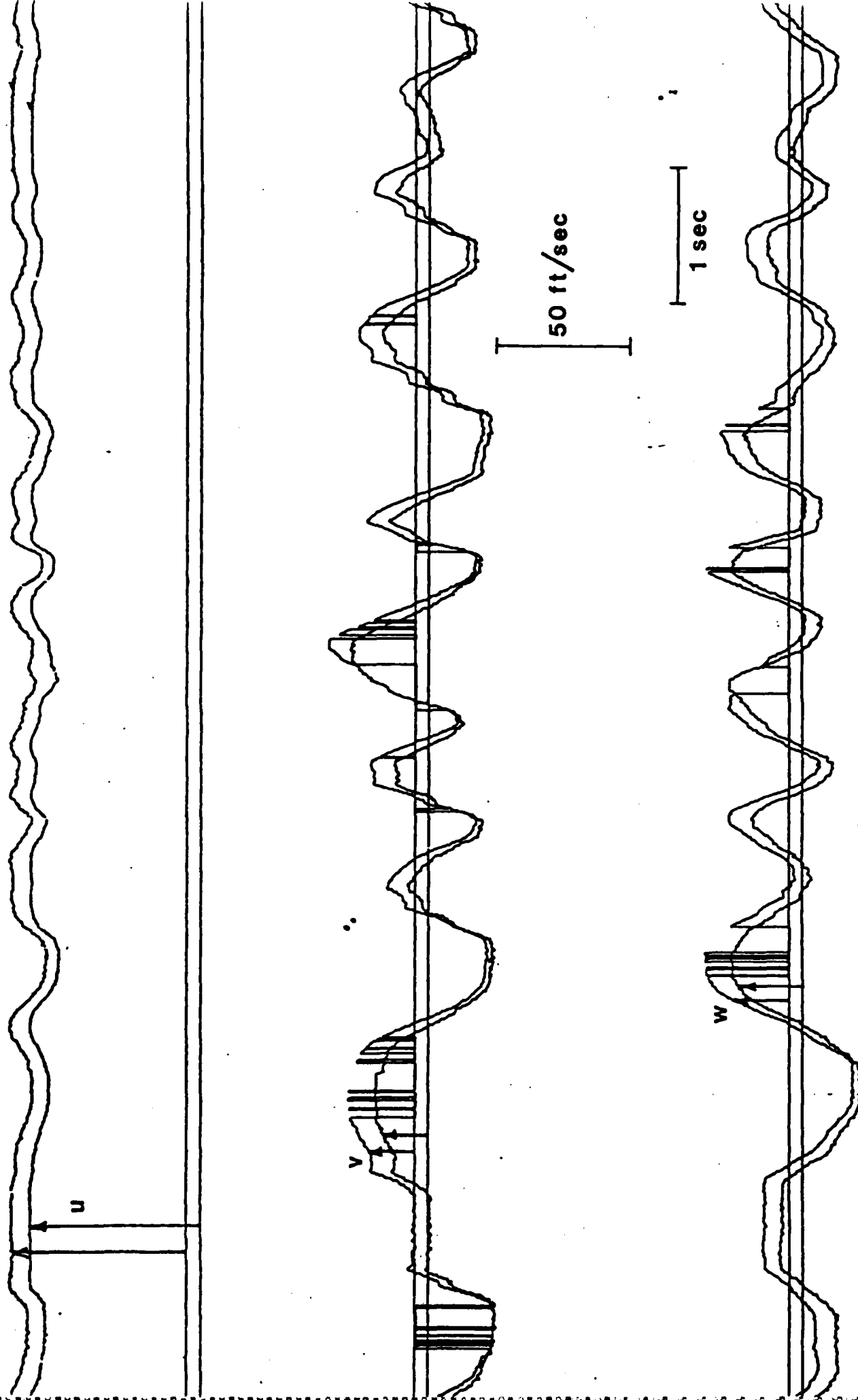


Fig. 15 Same data as shown in Fig. 13, with iteratively computed velocity component differing by more than 5 ft/sec from the correct value set to zero.

END

8-87

DTIC